

# Thermal Analysis of Polyimide-Cobalt Ferrite Nanocomposites

D. Mazuera<sup>\*</sup>, O. Perales-Pérez<sup>\*\*</sup>, B. Rentería<sup>\*\*</sup> and O. M. Suárez<sup>\*\*</sup>

<sup>\*</sup>University of Puerto Rico, Department of Mechanical Engineering, Mayagüez, Puerto Rico 00681

<sup>\*\*</sup>University of Puerto Rico, Department of Engineering Science and Materials, Mayagüez, Puerto Rico 00680-9044

## ABSTRACT

Thermal stability and thermomechanical behavior of a new polymer-based nanocomposite was conducted to assess the viability of its fabrication process. The nanocomposite films consisted of a polyimide matrix and dispersoids of 20nm cobalt ferrite single crystals exhibiting room-temperature coercivity of 2.9 kOe. For the sake of comparison, a bare polyimide film was also prepared. Infrared spectroscopy and x-ray diffraction analyses confirmed proper composite fabrication with development of expected phases. Dynamical mechanical analysis measurements of  $\tan \delta$  and storage modulus as a function of temperature evidenced an increase in the viscous-like behavior of the composite film by incorporation of the ferrite nanocrystals within the polymeric matrix. The corresponding reduction in the storage modulus values were validated by thermo-gravimetric analysis as a function of time and heating temperature in both, the bare polymer film and the nanocomposites.

**Keywords:** PMC, magnetic nanocomposite, cobalt ferrite, polyimide, thermal analysis.

## 1 INTRODUCTION

Polymer matrix magnetic composites and nanocomposites, commonly referred to as *magnetic polymers*, are receiving an increasing interest due to their wide range of potential applications: polymer bonded magnets, microelectromechanical systems (MEMS), microsensors, high density storage and magneto-optical media, electromagnetic shielding, cell separation, medical diagnosis, controlled drug delivery, etc [1-15]. Their relative low cost and light weight are appealing factors when compared to metallic or ceramic magnets. Their high formability and machinability, and the possibility of bearing outstanding magnetic properties due to the incorporation of nanosize dispersoids make these composites the material of choice to fabricate micro- or macro-scaled devices with the typical advantages of using polymer matrices [9, 16]. Regarding the disperse phase, it has been already demonstrated the possibility of tuning the magnetic properties of cobalt ferrite nanoparticles by a precise control on their crystal size within the single domain region. This type of control leads to outstanding

values of coercivity compared with typical values of the bulk [17] and enables this nanomaterial to be considered a suitable dispersoid in polymer-based composites for use in microelectronic and sensing devices [1, 5, 15]. However, since cobalt ferrite particles would behave as nanosize permanent magnets (because of its high coercivity and residual magnetic induction) they tend to cluster together making their homogeneous dispersion within the matrix a challenging task. In this work, 20 nm cobalt ferrite single crystals, which exhibited a coercivity of 2.9kOe at room-temperature, were used as dispersoids (10% and 20% ferrite volume fraction) in a polyimide matrix. A high spindle speed homogenizer was used to improve the dispersion conditions. The thermomechanical properties of the resulting nanocomposites were determined as a function of the volumetric load of the ferrite nanocrystals. The thermal stability and thermomechanical properties of the composite films were carried out by using thermo gravimetric analysis (TGA) and dynamical mechanical analysis (DMA), techniques. The obtained results were used to assess the feasibility of the nanocomposite fabrication.

## 2 EXPERIMENTAL

### 2.1 Materials

All reagents were of analytical grade and were used without further purification. Required weights of chloride salts of Fe(III) and Co(II) ions were dissolved in distilled water to achieve a mole ratio Fe/Co of two. NaOH was used as the precipitating agent. Commercial polyimide precursor (Dupont PI2555) and isopropyl trisostearyl titanate (Kenrich Prtrochemicals KR-TTS) were used as-received.

### 2.2 Synthesis of Cobalt Ferrite Nanocrystals

Cobalt ferrite nanocrystals were synthesized by a modified coprecipitation method. An aqueous solution of 0.11M Fe(III) and 0.55M Co(II) was continuously added by controlled flow rate into the reaction vessel containing an aqueous solution of 0.48M NaOH under boiling conditions. The vessel was heated for one hour to allow dehydration and atomic rearrangement involved with the conversion of the precursor hydroxide into the ferrite structure. Ferrite nanocrystals were magnetically decanted, washed

thoroughly three times with distilled water and dried in air at 80°C for 24 hours [17].

### 2.3 Fabrication of Polyimide-Cobalt Ferrite Nanocomposites

The polyimide precursor (Dupont PI2555) was previously treated with isopropyl trisostearyl titanate (KR-TTR) to help improving the dispersion of inorganic particles in polymeric matrices [3]. Ferrite powder was added to the solution and mixed using an IKA T18 homogenizer (with S18N-19G dispersing tool) for 1 hour of contact rotating at 10,000 RPM. The magnetic nanocomposites were prepared with 10% and 20% volumetric loads of ferrite nanocrystals.

### 2.4 Films Processing

Solvent-cast free-standing films of polyimide and the corresponding composites were prepared by pouring 0.6 to 1 ml of the precursor solution into a mold consisting of a glass substrate and a stainless steel ring (29.4 mm in diameter) that confined the solution into a circular shape. The mold containing the precursor solution was heated at 85°C until all solvent was removed. Produced films were peeled out from the substrate and thermally cured. This curing process was carried out by the following sequence: (i) heating of the films from room temperature to 200°C at a 4°C/min rate; (ii) 30 minutes of heating at 200°C; (iii) heating up to 300°C at 2.5°C/min; (iv) dwelling during 60 minutes; and (v) cooling down inside the furnace (furnace is turned off until room temperature is reached). The whole curing cycle took place in a 99.998% nitrogen atmosphere. The film thickness obtained ranged from 100µm to 150µm.

### 2.5 Structural Characterization

X-ray diffraction (XRD) and Fourier-transform infrared spectroscopy (FTIR) analyses were carried out to confirm the composite formation and the development of the expected phases (polymer matrix and disperse phase). XRD patterns were collected in a Siemens D500 x-ray diffractometer using the Cu-K $\alpha$  radiation while FTIR spectra were obtained in a Scimitar FTS 2000 Digilab spectrometer.

### 2.6 Thermal Analyses

Thermal stability tests were carried out by keeping the films at 400°C for 8h in a Mettler Toledo TGA 851e thermogravimetric analyzer. The same set-up was used to determine the degradation temperature of the films by heating them from room temperature to 600°C at 5°C/min. The viscoelastic behavior of the films was evaluated in a dynamical mechanical analyzer (Mettler Toledo DMA 861e) by measurements of  $\tan \delta$  (also known as tangent of the phase lag) and the storage (elastic) modulus  $M'$  as a

function of temperature for an applied 1Hz sine wave tensile load. The temperature was increased at a 5°C/min from room temperature to 400°C for these measurements.

## 3 RESULTS AND DISCUSSION

### 3.1 Structural Characterization

Figure 1 shows the FTIR spectra for bare polyimide and nanocomposite films with volumetric loads of ferrite nanocrystals of 10% and 20%. The bands at 1780  $\text{cm}^{-1}$ , 1710  $\text{cm}^{-1}$ , 1370  $\text{cm}^{-1}$  and 710  $\text{cm}^{-1}$  confirmed the presence of imide functional groups in the polymer. XRD analyses of the single components and nanocomposite, (Figure 2), also verified the formation of the expected polymeric and spinel (ferrite) structures.

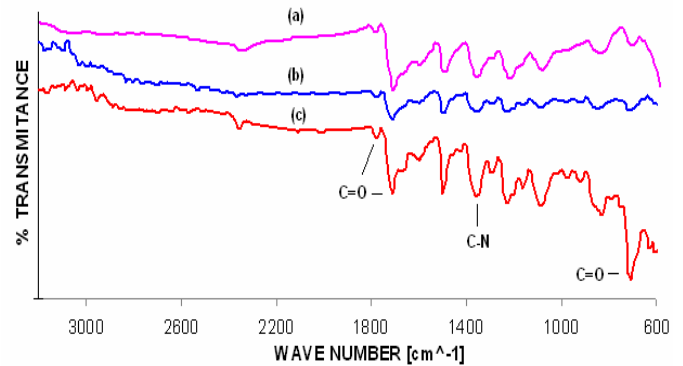


Figure 1. FTIR spectra for 20%v/v ferrite composite, (a); 10% v/v ferrite composite, (b); and polyimide films (c)

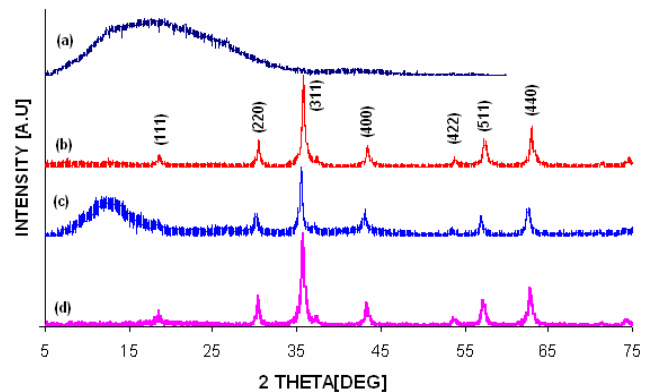


Figure 2. XRD patterns for bare polyimide film ,(a); pure cobalt ferrite powders, (b); 10% v/v ferrite composite, (c); and 20%v/v ferrite composite, (d)

### 3.2 Thermogravimetric Analyses

Thermogravimetric analysis (TGA) was used to determine the temperature of degradation (Figure 3) and the thermal stability as a function of time (Figure 4) of both, bare PI and nanocomposite films. Five percent of weight loss was set as the critical value, i.e. the maximum allowance in weight variation. The composite films experienced a pronounced weight loss, starting at 330°C, which became larger when the volumetric load of the ferrite increased from 10% to 20%. Bare PI film remained stable until 500°C (Figure 3). The thermal stability of the films was evaluated by determining the weight loss of the samples at a function of time at 400°C. The data shown in Figure 4, revealed an almost constant weight loss rate of the composite with heating time, which was more pronounced for a larger volumetric load of the ferrite phase (23% of weight loss after heating for 8 hours the nanocomposite with 20% v/v of ferrite). On the contrary, the bare PI film exhibited a negligible weight loss rate, evincing its high thermal stability. The weight loss in the nanocomposites could have been attributed to an incomplete imidization process; however, FTIR results did not show the presence of OH groups that would have reinforced this interpretation. Therefore, we should attribute the nanocomposite thermal behavior to a synergetic effect of chain scission, caused by the high centrifugal energy imposed of the homogenizer used to disperse the nanoparticles, and the presence of cobalt ferrite particles that hindered inter-chain bonding in the polyimide and hence, the final chains length. In order to confirm this hypothesis, a film of bare polyimide was produced after intensive homogenization, i. e. the same conditions used to prepare the composites. As Figure 3 evidenced, the PI film produced after intensive homogenization has an initial weight loss at 300°C (Figure 3-d), in contrast with 500°C observed when the PI film was produced without homogenization, (Figure 3-a).

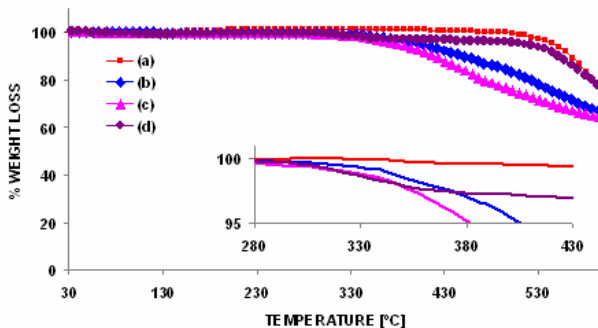


Figure 3. Degradation temperature for ‘non-homogenized’ bare polyimide, (a); 10% v/v ferrite composite, (b); 20%v/v ferrite composite, (c); and ‘homogenized’ bare PI films, (d)

### 3.3 Dynamical Mechanical Analyses

As Figure 5 evidences, composite films exhibited a reduction in storage (elastic) modulus,  $M'$ , compared to the value for bare polyimide. This reduction in  $M'$  value was larger as ferrite volume fraction in the film increased from 10% to 20%. Furthermore, the stepped profile of the  $M'$ -T plots corresponding to the composite films would suggest a molecular relaxation of the polymer matrix. Observed results were in agreement with the behavior observed in degradation and thermal stability tests, which suggested a lack in the development of polyimide microstructure due to the presence of ferrite nanocrystals in the composite.

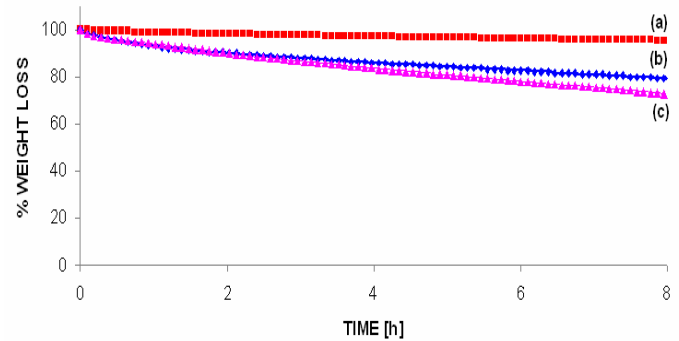


Figure 4. Degradation temperature for bare polyimide, (a); 10% v/v ferrite composite, (b); and 20%v/v ferrite composite films, (c).

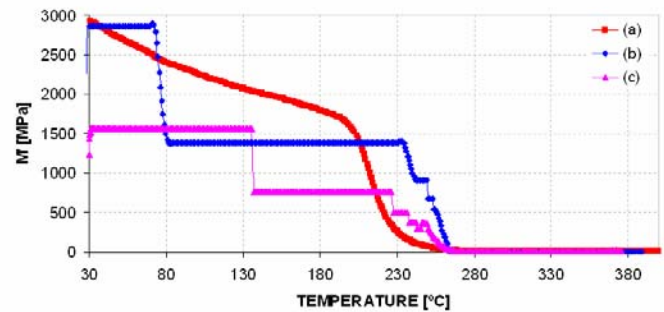


Figure 5.  $M'$  for bare polyimide, (a); 10% v/v ferrite composite, (b); and 20%v/v ferrite composite films, (c).

The variation of  $\text{Tan } \delta$  as a function of temperature, shown in Figure 6, suggested an increase in the viscous-like behavior for the composite films; an explanation also supported by the drop in  $M'$  values above discussed. Accordingly, the trends observed in Figures 5 and 6 indicate that an increment in the volumetric load of the disperse phase will lead to the rise in the  $\text{Tan } \delta$  values because, as mentioned before, the increase in nanoparticles volume fraction should have hindered the interchain binding. Furthermore, the observed dependence of  $M'$  and  $\text{Tan } \delta$  on the volumetric load of ferrite nanoparticles in the

films are in good agreement with their thermogravimetric behavior, discussed previously.

The glass transition temperature,  $T_g$ , of the various films was determined from the data shown in Figures 5 and 6. In Figure 6,  $T_g$  corresponds to the temperature at which a maximum value of  $\tan \delta$  was achieved. Accordingly,  $T_g$  values varied from 228°C in pure PI to 267°C in the composite films.  $T_g$  was also estimated as the onset of  $M'$  drop (Figure 5). In this later case,  $T_g$  varied from 205°C, in pure PI, to 230°C for both nanocomposites. This increase in the  $T_g$  values was attributed to the presence of solid particles (ferrite nanocrystals), which should have delayed the yielding process. The latter would also suggest an apparent matrix/dispersoids interaction when a stress is applied to the composite films. This load transfer mechanism, however, requires a more dedicated study that is beyond the scope of the present research.

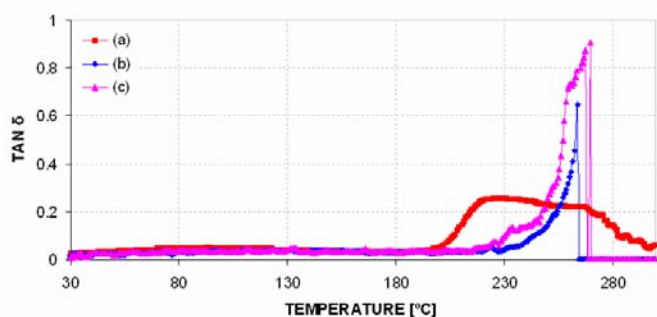


Figure 6.  $\tan \delta$  for bare polyimide, (a); 10% v/v ferrite composite, (b); and 20%v/v ferrite composite films, (c).

#### 4 CONCLUDING REMARKS

We have developed polyimide-based magnetic nanocomposite films with tunable mechanical, thermal-stability and magnetic properties. This tuning of the composite properties was attained by a suitable control of the processing conditions and the corresponding volumetric load of the ferrite nanocrystals within the polymeric matrix. Our results suggest that polyimide-ferrite nanocomposites can be used without any concern about their physical and structural stability for applications involving temperatures up to 80°C. Higher temperatures would be conducive to decrease in both, mechanical properties and the corresponding thermal stability.

#### ACKNOWLEDGMENTS

This material was based upon work supported by the National Science Foundation under award N° DMR.0351449 (PREM Program). Thanks are also extended to Kenrich Petrochemicals and HD Microsystems for assistance and technical support.

#### REFERENCES

- [1] Tsung-Shune Chin, *Journal of Magnetism and Magnetic Materials*, 209, 75-79, 2000.
- [2] L. García-Cerda, M. Escareño-Castro, M. Salazar-Zertuche, *Journal of Non-Crystalline Solids*, 353, 808–810, 2007.
- [3] L. Lagorce, M. Allen, *Journal of microelectromechanical systems*, vol. 6, no. 4, 307-312, 1997.
- [4] K. Baba, F. Takase, M. Miyagi, *Optics Communications*, 139, 35-38, 1997.
- [5] S. Spearing, *Acta mater*, 48, 179-196, 2000.
- [6] C. P. Sasso, M. Pasquale, L. Giudici, S. H. Lim, S.M. Na, *Sensors and Actuators*, 129, 159–162, 2006.
- [7] A. Voigt, M. Heinrich, C. Martin, A. Llobera, G. Gruetzner, F. Pérez-Murano, *Microelectronic Engineering*, 84, 1075–1079, 2007.
- [8] S. Sindhua, S. Jegadesanb, A. Parthibanb, S. Valiyaveettil, *Journal of Magnetism and Magnetic Materials*, 296, 104–113, 2006.
- [9] M. Makleda, T. Matsuib, H. Tsudab, H. Mabuchib, M. El-Mansya, K. Morii, *Journal of Materials Processing Technology*, 160, 229–233, 2005.
- [10] S. K. Lim, K. J. Chung, Y. Kim, C. K. Kim, C.S. Yoon, *Journal of Colloid and Interface Science*, 273, 517–522, 2004.
- [11] I. G. Yanez-Flores, R. Betancourt-Galindo, J. A. Matutes Aquino, O. Rodriguez-Fernandez, *Journal of Non-Crystalline Solids*, 353, 799–801, 2007.
- [12] J. H. Kim, J. Kim, K. H. Baek, D. H. Im, C. K. Kim, C. S. Yoon, *Colloids and Surfaces A: Physicochem. Eng. Aspects*, 301, 419–424, 2007.
- [13] J. Zhan, G. Tian, L. Jiang, Z. Wu, D. Wu, X. Yang, R. Jin, *Thin Solid Films*, 916, 6315-6320 2008.
- [14] J. Slama, A. Gruskova, R. Vıcen, S. Vıcenova, R. Dosoudil, J. Franek, *Journal of Magnetism and Magnetic Materials*, 254–255, 642–645, 2003
- [15] M. Pasquale, C. P. Sasso, M. Velluto, S. H. Lim, S.H, *Journal of Magnetism and Magnetic Materials*, 242–245, 1460–1463, 2002.
- [16] D. Askeland, P. Phule, *The science and engineering of materials*, Fifth Edition, Thomson, 2005.
- [17] Y. Cedeño-Mattei, O. Perales-Pérez, M. Tomar, F. Román, *Journal of Applied Physics*, 103, 07e512, 2008.
- [18] P. M. Ajayan, L. S. Schadler, P. V. Braun, *Nanocomposite Science and Technology Wiley-Vch*, 2003.